NANOSTRUCTURE MECHANISM OF FORMATION OF OXIDE FILM IN HEAT-RESISTANT Fe – 25Cr – 35Ni SUPERALLOYS

S. Yu. Kondrat'ev,[1] G. P. Anastasiadi,[1] and A. I. Rudskoy[1]

High-temperature oxidation of heat-resistant alloys based on the Fe – Cr – Ni system is investigated. Alloy 25% Cr – 35% Ni – C – Si – Nb is used as an example to show the nanoscale level of the oxidation process. The nature of the process and its kinetics are determined.

Key words: cast heat-resistant refractory alloys, microstructure, phase composition, high-temperature oxidation, selective oxidation of phases.

INTRODUCTION

Oxidation of heat-resistant steels and alloys operating at a high temperature determines largely the service life of the equipment produced from them. The oxidation behavior depends on the chemical composition of the alloy and on its structure, which makes prediction of the operating capacity of alloys with multiphase structure a difficult task due to the substantial evolution of the structure during operation.

For example, the initial cast structure of HP-modified heat-resistant alloys of the Fe – Cr – Ni – C – Si – Nb system includes a stable matrix γ-phase based on Fe – Cr – Ni (up to 90 vol.%), an eutectic arranged on the boundaries of dendrite cells and represented by a chromium-base carbide (M_7C_3 or $M_{23}C_6$) and the matrix phase, and a niobium carbide (NbC) uniformly distributed in the matrix [1, 2]. The behavior of the different initial and intermediate phases in the structure of the alloys of this system [3 – 5] under a long high-temperature hold in an environment containing oxidants (air, O_2, CO, CO_2, etc.) differs markedly [6 – 9]. In accordance with the level of the resistance to oxidation the phases in the alloys in question may be arranged in the following series: chromium-base carbides, matrix, intermediate phases, niobium-base carbides. Another possible process is internal oxidation of the active elements (silicon, titanium, aluminum, chromium, etc.), when oxygen anions diffuse through the scale film into the alloy. Simultaneously, the highly volatile elements (chromium, manganese and others)

evaporate intensely at a high temperature into the ambient. This disturbs substantially the initial optimum proportion of the chemical components in the alloy and lowers its resistance to oxidation. The destruction and breakage of the scale under long-term oxidation under thermal cycles in operation results in formation of higher oxides in the scale; for chromium they correspond to the stoichiometric composition of CrO_2 and CrO_3 with a high volatility. In some cases this may lead to catastrophic oxidation and removal of a part of the mass of the metal into the ambient [6, 9, 10]. It has been shown [8, 10, 11] that the process of formation and removal of oxides in the forming scale develop in volumes 20 – 100 nm in size. Depending on the proportion of the rates of these processes the mass in a local volume may grow or be lost.

The main requirement on refractory alloys is the operating capacity of articles produced from them under intense interaction with the ambient and in operating media of various compositions and chemical activities. Modern petrochemical productions require elevation of the permissible temperature of pyrolysis of the hydrocarbon materials, which is accompanied by local overheating of the functional zones of efficient plants [12, 13]. This makes it necessary to study the processes of oxidation of Fe – Cr – Ni-base alloys in the temperature range of 1100 – 1200°C.

The aim of the present work was to study the process of oxidation of alloy Fe – 25% Cr – 35% Ni – C – Si – Nb at a temperature of 400 – 1150°C and to estimate its high-temperature strength under the conditions of operation of high-temperature pyrolysis units in the petrochemical industry.

---

[1] St. Petersburg Polytechnic University, St. Petersburg, Russia (e-mail: petroprom2013@yandex.ru).
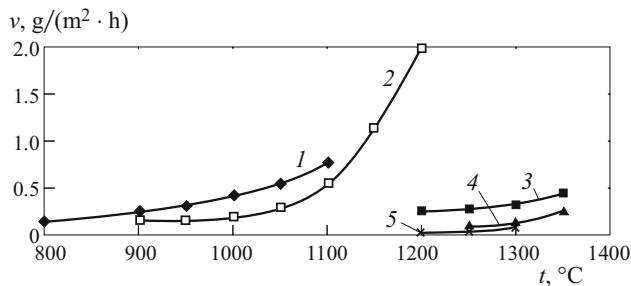
Fig. 1. Dependence of the rate of oxidation in air on the temperature for alloys of the Fe – Cr – Ni-base system: *1*) 36Kh18N25S2 [15]; *2*) 45Kh26N33S2B2 (the object of our study); *3, 4, 5*) 10Kh16N45Yu3 [15] (for the oxidation time of 100, 500, and 2000 h, respectively).

Fig. 2. Dependence of the rate of oxidation in air *v* on the duration of the hold at 1200 – 1350°C for alloy 10Kh16N45Yu3 [15].

METHODS OF STUDY

We studied refractory alloy Fe – 0.45% C – 26% Cr – 33% Ni – 2% Si – 2% Nb used for making radiant coils of high-temperature pyrolysis units [14]. The alloy was melted in an induction furnace with capacity 500 kg from pure blend materials and cast into sand molds for standard wedge samples (GOST 977–88). The actual chemical composition of alloy 45Kh26N33S2B2 was as follows (in wt.%): 0.46 C, 1.73 Si, 1.31 Mn, 25.5 Cr, 35.6 Ni, 1.60 Nb, 0.59 W, 0.31 Mo, 0.21 Ti, 0.05 N, the remainder Fe.

The kinetics of the oxidation of the alloy was studied with the help of a facility combining thermogravimetric analysis with differential scanning calorimetry (TGA/DSC 1/1600 HF, "Mettler-Toledo AG," Switzerland). To study the temperature dependence of the oxidation rate of the alloy we used specimens in the form of chips 0.2 – 0.4 mm thick with an initial mass of 73.014 mg; the rate of air heating was 1 K/min in a temperature range of 900 – 1200°C. The oxidation kinetics at a constant temperature of 900°C was studied on flat specimens $48 \times 8 \times 4.5$ mm in size with an initial mass of 14.0777 g. The accuracy of the measurement of the mass was 0.0001 g. The metallographic analysis of the structure after oxidation in an air atmosphere and in vacuum was performed on specimens $10 \times 10 \times 15$ mm in size. The tests were performed in a vacuum chamber with water cooling and a tungsten heater. The device kept vacuum at a level of $133 \times (10^{-2} – 10^{-3})$ Pa. The temperature was controlled by a thermocouple of type VR (W – Re). The accuracy of the measurement of the temperature was ± 2°C. We measured the thickness of the oxidized layer after a high-temperature hold at 400 – 1150°C in an air environment or in vacuum. We also studied the variation of the structure, the phase composition of the alloy, and the distribution of the chemical elements over the thickness of the layer.

The microstructure of the alloy was studied under a Carl Zeiss Axiovert 40 light metallographic microscope at a magnification of $\times 50 – 1000$ using a program for automatic quantitative analysis of images in accordance with
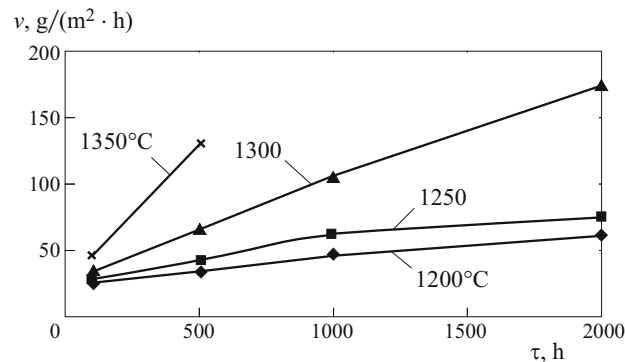
ASTM E 1245-03. The laps were prepared using a "Buehler" device according to ASTM E 3-95. To uncover the structure we subjected the specimens to electrolytic etching in 10% oxalic acid. The structure of the surface of the alloy was studied under a Quanta 200 3D FEG scanning electron microscope.

The x-ray spectrum analysis of the distribution of elements in the matrix and of the phase composition was performed using a Tescan VEGA 5136 LM device with 3% accuracy of the determination of the concentration of Fe, Ni, Cr, Si, Nb, Mo, W, and Ti and 20% accuracy of the determination of the concentration of C and N (in relative units).

RESULTS AND DISCUSSION

Figure 1 presents the results of the evaluation of the rate of oxidation in air for several alloys based on the Fe – Cr – Ni system. It can be seen that the rate of the oxidation depends substantially on the carbon content. For example, alloy 10Kh16N45Yu3 has a high resistance to oxidation until 1300°C. The oxidation rate of the alloys with a medium carbon content (0.4 – 0.5 wt.%) is higher by about a factor of 10, but the effect of the carburization (saturation of the alloy with carbon) under the action of the pyrolysis products on their mechanical properties and long-term operating capacity is substantially lower than in the alloys with a low carbon content (less than 0.10 wt.%).

It should be noted that the most oxidation-resistant alloy 10Kh16N45Yu3 passes from a parabolic mode of oxidation to a linear one in the temperature range of 1250 – 1300°C [15] (Fig. 2). This is explainable by the high volatility of chromium. At 1300°C the vapor pressure (p) attains 1.071 Pa for chromium, 0.557 Pa for iron, and 0.027 Pa for nickel in accordance with the equation $\log p = a + b/T + c \log T$ [16].

Quantitative determination has shown that the corrosion rate of alloy 45Kh26N33S2B2 at 1200°C is $v = 2.0$ g/(m² · h) (Fig. 3). This value is about two orders of magnitude higher than for the standard conditions of growth of Cr_2O_3 oxide on the surface of pure metal [6]. This means that it is necessary
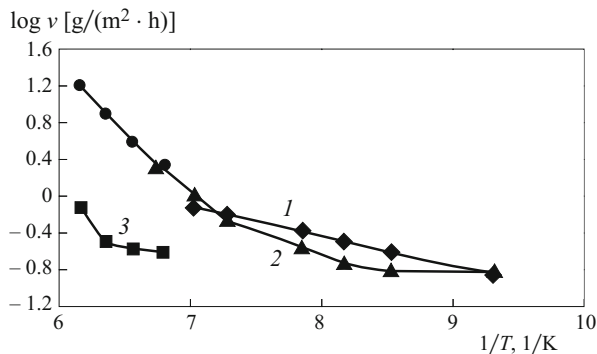
Fig. 3. Function $\log v = f(1/T)$ for heat-resistant alloys: *1*) 36Kh18N25S2 [15]; *2*) 45Kh26N33S2B2 [△) experiment, ●) prediction]; *3*) 10Kh16N45Yu3 [15].

Fig. 4. Dependences of the gain in mass Δm on the time of oxidation for cast alloy 45Kh26N33S2B2 at 900°C: *a*) in the three (*I, II, III*) oxidation periods; *b*) in the first stage; *1*) experimental results; *2*) computation by the parabolic law of growth of the thickness of oxide film $\Delta m = 0.0030\tau^{0.5}$.

to estimate the effect of corrosion on the operating capacity of the equipment produced from alloy 45Kh26N33S2B2 in advance for the specified operating conditions.

The high rate of corrosion of alloy 45Kh26N33S2B2 seems to be explainable by the enhanced defectiveness of the scale formed on the surface of the alloy and by the accelerated transport of oxygen through it. Growth in the temperature and in the number of defects in the structure of the scale may result in formation of excess oxygen, when the oxidation of the scale is more intense, and volatile higher oxides form by the reaction

$$Cr_2O_3 + O \rightarrow 2CrO_2\uparrow \ \ or \ \ Cr_2O_3 + 3O \rightarrow 2CrO_3\uparrow.$$
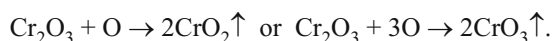
The oxide evaporates into the environment, which destroys the scale, and the oxidation mode becomes catastrophic and is accompanied by a loss (removal) of the mass of the specimen.

For a more detailed analysis of the high-temperature oxidation behavior of alloy 45Kh26N33S2B2 we studied its oxidation under an isothermal hold in air at 900°C. The alloy was oxidized in three stages, the first of which lasted for 40 min, the second for 110 min, and the third for 200 min. After each stage the specimen was cooled with the furnace to room temperature. This mode of oxidation imitates an operating regime including a start and a stop of the equipment, when the thermal cycles affect substantially the formation of the scale structure and the appearance of defects in the latter. The temperature mode was maintained automatically. During the isothermal hold the specimen was weighed at a step of 30 – 60 sec. The results of the test were used to recalculate the gain in the mass of the specimen into the conventional scale thickness by the relation $\delta \approx \Delta m/(\gamma S_0)$, where Δm is the gain in the weight (g), $\gamma = 8.15$ g/cm^3 is the density of the alloy, and $S_0 = 12.72$ cm^2 is the area of the surface of the specimen. The experimental results (Fig. 4*a*) allow us to divide the oxidation process of alloy 45Kh26N33S2B2 at 900°C conventionally into several stages. The first stage (the 40-min oxidation) corresponds to the most intense initial oxi-
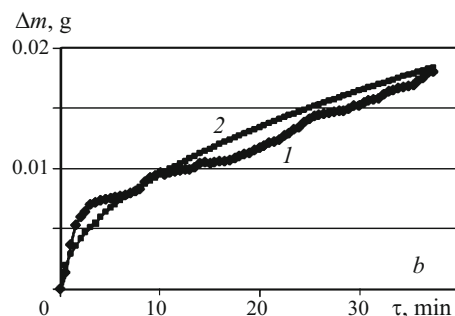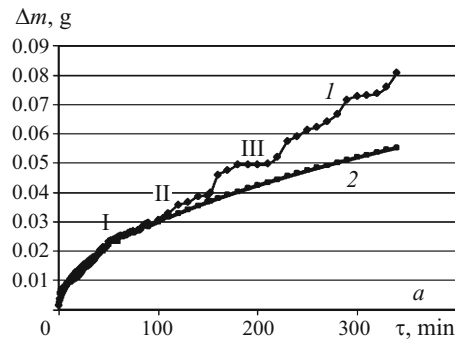
dation of the alloy, after which the total thickness of the scale is $\delta \approx 1.72$ μm. In the second stage (at a total oxidation time of about 150 min) the oxidation process obeys a parabolic law, which means that the Cr_2O_3 film has a quite dense structure. In this case the oxidation is accompanied by diffusion of oxygen to the surface of the alloy; the oxygen flow decreases with growth of the thickness of the scale, which attains $\delta \approx 3.83$ μm after the second stage of the process. In the third stage the gain in the mass of the specimen is somewhat higher, than it should be in accordance with the parabolic oxidation law. The rate of the oxidation in this stage fluctuates. This seems to be connected with the changes in the structure of the scale upon growth of its thickness, which attains $\delta \approx 6.71$ μm after the third stage. It is known [17] that a chromium oxide film with a thickness exceeding 3 μm formed on the surface of an alloy has a porous structure. Such a film does not reduce the flow of oxygen through it to the surface of the alloy and does not decelerate the growth of the scale.

The first stage of the initial oxidation (Fig. 4*b*) may also be divided into three periods, i.e., (*I*) accelerated oxidation for $0 – 2$ min (the film acquires a thickness $\delta \approx 0.63$ μm), (*II*) deceleration of the process and start of the mode of parabolic oxidation ($\Delta m = 0.0030\tau^{0.5}$) for $2 – 8$ min ($\delta \approx 0.72$ μm), and (*III*) parabolic oxidation for $8 – 40$ min.

Accelerated initial oxidation ($0 – 2$ min) of a ground surface with surface finish $5 – 7$ (roughness class $11 – 12$, mean
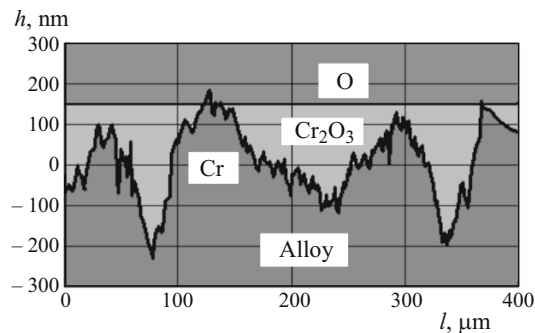
Fig. 5. Profile of a ground surface of alloy 45Kh26N33S2B2 and mechanism of filling of depressions with Cr_2O_3 oxide (diagram).

height of profile irregularities $R_z \approx 100$ nm) is determined by considerable growth of the area of the profile of the specimen with respect to the plane of the oxygen flow under oxidation (Fig. 5). In addition, oxidation on a surface with nanosize protrusions, slopes and depressions produced by mechanical treatment should occur more intensely due to the considerable plastic straining of surface volumes. In the second period (2 – 8 min) of the initial stage of oxidation, when the depressions of the profile are filled with the forming Cr_2O_3 oxide (Fig. 5), the growth rate of the oxide decreases markedly due to the reduction of the flow of oxygen through the scale until the oxidation mode attains a parabolic pattern in the period of 8 – 40 min (Fig. 4b).

The experimental results obtained agree well with the data of the authors of [10], who seem to be pioneer researchers of the early stages of oxidation at relatively low temperatures (500 – 600°C) and a short-term hold (10 min) in a controlled oxygen environment at $10^{-4} - 10^{-2}$ Pa ($10^{-9} - 10^{-7}$ atm) for alloy Ni – 18% Cr chosen as an example. It is shown in [10] that spherical nickel-base oxide inclusions ("nodules") form on the surface of the alloy in the early oxidation stages; later on nickel is substituted by chromium. The diameter of the particles is about 300 nm. Repeated oxidation causes formation of particles of a "second generation" virtually without growth of the primary oxides. Simultaneously, micropore-like structures ("holes"), also about 300 nm in size, form near the oxide particles. In the zone of their interface with the solid solution the content of the main chemical elements of the alloy (nickel and chromium, as well as oxygen) changes substantially. This process always occurs in refractory alloys under primary heating and produces a thin layer of scale. Such a layer (given that it is stable) protects the metal from accelerated oxidation and transfers the process to an oxidation mode limited by the transport, i.e., the diffusion, of oxygen through the scale and of metal to the place of formation of the oxide. The scale is represented by numerous randomly oriented grains up to 300 nm in size formed from individual centers. The diffusion penetrability of the oxide to grain boundaries is considerably (by orders of magnitude) higher than over the volume. A local excess of oxygen can raise the degree of oxidation of the Cr_2O_3 oxide

and produce a volatile $CrO_2\uparrow$ compound and pores. A regular low-defective crystal oxide structure forms only when the processes of the appearance and growth of the pores are controlled.

The experimental results obtained and their comparison with the data of [10] allow us to describe the mechanism of high-temperature oxidation of alloy 45Kh26N33S2B2 as follows.

The first (initial) stage of oxidation of the alloy is an unsteady process; by the data of [10] in the first 10 min the surface of the alloy is "inhabited" by oxide particles with a size of about 300 nm. Separate oxides form on the surface of several protrusions, slopes and depressions (Fig. 5), and the kinetics of their growth is not related to the transport of oxygen to the oxide-forming element, i.e., chromium. The rate of growth of the mass in the first 2 min is very high (Fig. 4). When the surface of the alloy is covered with an oxide film (in up to 8 min), the mass of the specimen changes little. After 8 min of the hold at 900°C, the oxidation process acquires an unsteady mode due to the action of different mechanisms, namely,

(*1*) the diffusion flow through the scale (chiefly C_2O_3) to the surface of the alloy decreases with growth of the scale thickness, and the rate of growth of the mass decreases;

(*2*) the oxygen accumulated in the surface layer of the scale interacts with the chromium oxide by reactions $Cr_2O_3 + O \rightarrow 2CrO_2\uparrow$ or $Cr_2O_3 + 3O \rightarrow 2CrO_3\uparrow$ that yield volatile oxides emitted from the scale to the ambient, which results in formation of pores in the oxide layer and makes the scale more penetrable for oxygen. This accelerates the formation of the Cr_2O_3 oxide in the scale (near the surface of the alloy and in the bulk of the scale);

(*3*) filling of the pores with the Cr_2O_3 oxide again reduces the flow of oxygen to the surface of the alloy and hence the gain in the mass of the specimen.

The process described can be traced in Fig. 4b with respect to the computed curve of parabolic oxidation $\Delta m = k\tau^{0.5} = 0.0030\tau^{0.5}$, g/min. The curve of the actual gain in the weight in stage *I* mostly goes below the theoretical oxidation curve.

In ***the second stage*** of oxidation of a specimen (under the second heating) (Fig. 4a) the curve describing the gain in the weight is located somewhat lower than the theoretical one.

In ***the third stage*** of oxidation (after about 150 min of the total hold at 900°C) (Fig. 4a) the gain in the mass is much higher than the theoretical value of the parabolic law ($\Delta m = 0.0030\tau^{0.5}$). For the interval of 153 – 340 min of the oxidation process in the third stage the theoretical gain in the weight is 0.018 g, while the experimental value is 0.041 g. This is an indirect evidence of a substantial content of flaws in the structure of the scale formed in the late stages of oxidation of alloy 45Kh26N33S2B2, which increases its rate substantially. A similar behavior of the oxidation curve has been reported in [18] in a thermogravimetric study of steel
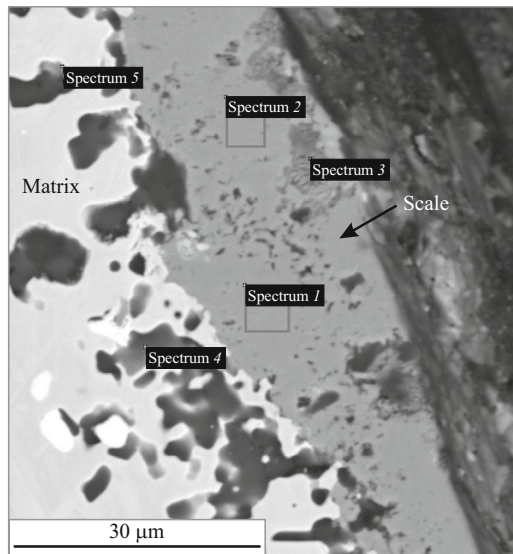
Fig. 6. Microstructure of scale and of oxidized surface layer of cast alloy 45Kh26N33S2B2 after a 565-h hold at 1150°C at a stress of 6 MPa in air (SEM).

Fig. 7. Content of oxygen in the phases present in the structure of cast alloy 45Kh26N33S2B2 after high-temperature oxidation at different temperatures in vacuum (400, 600 and 800°C) and in air (600, 800 and 1150°C): *1* (▲)) niobium carbide; *2* (◆)) matrix; *3* (●)) γ'-phase; *4* (■)) chromium carbide.

TP347 (Fe – 18% Cr – 10% Ni – 0.5% Nb) in air at 750°C including the different stages and periods of the process.

The metallographic and microscopic x-ray spectrum analyses of surface layers of alloy 45Kh26N33S2B2 after a hold at 400 – 1200°C have shown that oxidation of the ally is a complex process connected with its multiphase structure. The presence of several phases with substantially different chemical compositions in the cast structure and their evolution under a high-temperature hold [1 – 5] determine the selective oxidation behavior.

Our experimental data show that different phases are oxidized in the surface layer of the alloy under the oxide film with different intensity (Fig. 6). The least stable phase in the structure is the niobium carbide, while the γ-solid solution, the intermediate intermetallic phases and the chromium carbides are relatively resistant to oxidation until 1150°C (Fig. 7).

CONCLUSIONS

Investigation of the processes of high-temperature oxidation of heat-resistant refractory alloys based on the Fe – Cr – Ni system is a necessary aspect of determination of their operating capacity under operation. The oxidation process develops at a nanosize level (up to 300 nm) and is determined by the kinetics of the high-temperature oxidation of the alloy, of the formation of scale from stable (Cr_2O_3) and volatile (CrO_2) oxides, of the degradation of the structure of the scale and of the related "fluctuating" processes of growth of the mass of the specimens observed by the methods of thermal gravimetry. Analysis of experimental data shows that the rate of corrosion of multiphase alloys based on the Fe – Cr – Ni system depends on the physicochemical, production and operation parameters. This creates difficulties
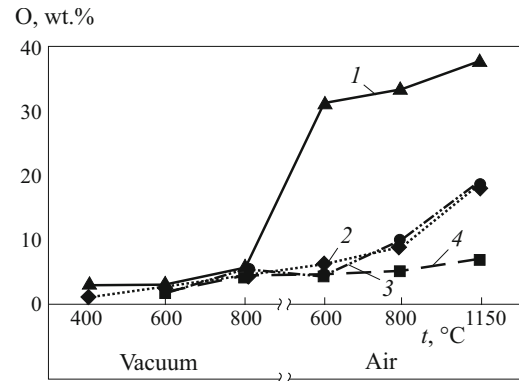
with prediction of the operating capacity of the high-temperature equipment produced from them under various operating conditions. Thus, preliminary tests of their corrosion resistance should be performed for evaluating the service life of heat-resistant refractory alloys in every specific case. It is important not only to determine the quantitative parameters of the oxidation but also to study the nature of the corrosion damage and its effect on the mechanical properties of the alloy.

REFERENCES

1. A. I. Rudskoy, A. S. Oryshchenko, S. Yu. Kondrat'ev, et al., "Special features of structure and long-term strength of cast refractory alloy 5Kh26N33S2B2," *Metalloved. Term. Obrab. Met.*, No. 4(694), 42 – 47 (2013).
2. A. I. Rydskoy, A. S. Oryshchenko, S. Yu. Kondrat'ev, et al., "Mechanism and kinetics of phase transformations in refractory alloy 45Kh26N33S2B2 under long high-temperature holds. Part 1," *Metalloved. Term. Obrab. Met.*, No. 1(703), 3 – 8 (2014).
3. A. S. Oryshchenko, S. Yu. Kondrat'ev, G. P. Anastasiadi, et al., "Special features of structural changes in refractory alloy 45Kh26N33S2B2 at operating temperatures. Report 1: Cast state," *Nauch.-Tekh. Vedomosti SPbGPU, Ser. "Nauka Obraz."*, No. 1(142), 155 – 163 (2012).
4. A. I. Rudskoy, S. Yu. Kondrat'ev, G. P. Anastasiadi, et al., "Mechanism and kinetics of phase transformations in refractory alloy 45Kh26N33S2B2 under long high-temperature holds. Part 2," *Metalloved. Term. Obrab. Met.*, No. 3(705), 12 – 19 (2014).
5. A. I. Rudskoy, G. P. Anastasiadi, S. Yu. Kondrat'ev, et al., "Effect of the factor of the number of electron vacancies on the kinetics of formation, growth, and dissolution of phases under long high-temperature holds of refractory alloy 0.45C – 26Cr – 33Ni – 2Si – 2Nb," *Fiz. Met. Metalloved.*, **115**(1), 3 – 13 (2014).
6. N. Birks and G. Meier, *An Introduction into High-Temperature Oxidation of Metals* [Russian translation], Metallurgiya, Moscow (1987), 184 p.

7. H. Asteman, J. Svensson, and L. Johansson, "Oxidation of 310 (25/20) steel in H_2O/O_2 mixture at 600°C. Effect of water-vapor-enhanced chromium evaporation," *Corrosion Sci.*, **44**, 2635 – 2649 (2002).

8. C. Ostwald and H. Grabke, "Initial oxidation and chromium diffusion. Effects of surface working on 9 – 20% Cr steels," *Corrosion Sci.*, **46**, 1113 – 1127 (2004).

9. R. F. Voitovich, *Oxidation of Carbides and Nitrides* [in Russian], Naukova Dumka, Kiev (1981), 192 p.

10. N. McIntyre, N. Chan, and C. Chen, "Characterization of oxide structures on nickel-chromium alloy during low pressure oxidation at 500 – 600°C," *Oxidation Met.*, **33**(5 – 6), 458 – 479 (1990).

11. C. L. Angerman, "Long-term oxidation of superalloys," *Oxidation Met.*, **5**(2), 149 – 167 (1972).

12. A. Oscar Quintana Ponce, *Structural and Magnetic Studies of an Ex-Service Cast Austenitic Steel Tube Used in Hydrogen Preformers, Author's Abstract of Doctoral's Thesis*, Chicago, Illinois (2012), 176 p.

13. D. J. Tillack and J. E. Guthrie, "Wrought and cast heat-resistant stainless steels and nickel alloys for the refining and petrochemical industries," *Nickel Development Inst., Toronto, Technical Ser.*, No. 10, 71 – 85 (1998).

14. A. S. Oryshchenko, "Structural materials for radiant coils of high-temperature units of the petrochemical industry," *Metallurg*, No. 2, 66 – 68 (2008).

15. S. B. Maslenkov and E. A. Maslenkova, *Steels and Alloys for High Temperatures, In Two Books, Book 1* [in Russian], Metallurgiya, Moscow (1991), 384 p.

16. D. R. Lide, "Properties of the elements and inorganic compounds: Vapor pressure of the metallic elements," in: *Handbook of Chemistry and Physics, 84 Ed., Online Version*, CRC Press, Boca Raton, Florida (2003), Section 4, pp. 4-1 – 4-166.

17. A. A. Kaya, P. Krauklis, and D. J. Young, "Microstructure of HK40 alloy after high-temperature service in oxidizing/carburizing environment. I. Oxidation phenomena and propagation of a crack," *Mater. Characteriz.*, **49**(1), 11 – 21 (2002).

18. V. B. Trindade, U. Krupp, B. Hunjari, et al., "Effect of alloy grain size on the high-temperature oxidation behavior of the austenitic steel TP347," *Mater. Res.*, **8**(4), 35 – 41 (2005).